Original scientific paper

Informacije MIDEM
Journal of Microelectronics,
Electronic Components and Materials
Vol. 43, No. 2(2013), 97 – 102

Cylindrical-parabolic reflector with printed antenna structures

Aleksandar Nešić[1], Ivana Radnović[1], Marija Milijic[2], Zoran Mićić[1] and Dusan Nešić[3]

[1]Institute IMTEL Komunikacije a.d, New Belgrade, Serbia
[2]Faculty of Electronic Engineering, University of Nis, Nis, Serbia

[3]IHTM-CMTM, University of Belgrade, Belgrade, Serbia

Abstract: The paper presents concept of design and realization of the new class of printed antenna structures which consist of a linear axial array of dipoles, subreflector, feed network and a bal-un, all printed on a common dielectric substrate. The array is positioned on the axis focus of the cylindrical-parabolic reflector. Use of the reflector enables reducing back side radiation and shaping beamwidth in H-plane thus obtaining higher gain while the printed subreflector gives the possibility of achieving additional gain. Besides, by using dipoles with pentagonal shape that operate on the second resonance, enhanced bandwidth of the array has been accomplished. Four variants of such arrays have been realized: two of them with 8 radiating elements for the frequency range around 26 GHz – one with uniform and the other with tapered feed distribution, featuring gains of 27.5 dBi and 25.7 dBi, respectively. The latter has the side lobe suppression of 28 dB in E-plane. Two other arrays that are intended for ranges around 23 GHz and 60 GHz have 16 radiating elements, uniform feed distribution and measured gains of 33 dBi and 34 dBi, respectively. Bandwidths of all realized model for S11 less than -10 dB is around 30 %. In all cases agreement between simulated and measured results is very good.

Key words: Microwaves and millimeter waves, Antenna array, Printed antenna, Cylindrical-parabolic reflector

Cilindrično parabolični odbojniki s tiskanimi antenam

Povzetek: Članek predstavlja koncept dizajna in realizacijo nove tiskane antene, ki je sestavljena z linearno matriko dipolov, odbojnikom in napajalnim omrežjem na skupnem dielektričnem substratu. Niz je nameščen v žariščni osi cilindričnega paraboličnega odbojnika. Uporaba odbojnika omogoča znižanje sevanja nazaj in oblikovanje pasovne širine v ravnini H za doseganje večjega ojačenja Uporaba dipolov v obliki peterokotnika in delovanju v drugi resonančni frekvenci omogoča povečanje pasovne širine. Realizirane so štiri inačice teh matrik. V vseh primerih je bilo doseženo dobro ujemanje med simulacijami in meritvami.

Ključne besede: mikrovalovi in milimeterski valovi, matrična antenna, tiskana antenna cilindričen paraboličen odbojnik

* Corresponding Author's e-mail: nesicad@nanosys.ihtm.bg.ac.rs

1 Introduction

In the last two decades printed antenna structures are dominant over conventional antennas especially in microwave and millimeter wave ranges, except in some specific applications. They are practically indispensable in the field of reconfigurable antennas. Main advantages of printed antenna structures are: high reproducibility, small dimensions, low weight, compactness, beam scanning possibility as well as possibility of integration with passive and active microwave circuits.

However, there are applications where printed antennas show certain disadvantages such as: applications in high power transmitters (possibility of dielectric breakdown), applications in high gain antennas (due to relatively high losses in printed feed lines) and in antennas with very high side lobe suppression (over 40 dB) due to critical dimension tolerances.

In order to overcome these significant disadvantages, the concept of linear axial antenna array positioned on a focal axis of a cylindrical-parabolic reflector is introduced [1-4].

As radiating elements in the antenna array printed dipoles of pentagonal shape operating on the second resonance are used. In this way a much wider bandwidth than with conventional printed antenna arrays is obtained.

The presence of the cylindrical-parabolic reflector introduces a third dimension in a standard planar structure, and this is practically the only drawback comparing to conventional printed antenna arrays. However, by applying a subreflector which consists of two strips printed on both sides of the dielectric substrate, the depth of the cylindrical-parabolic reflector can be reduced and so the overall size of the antenna structure decreased.

Differently from Cassegrain antennas where subreflector covers the central part of the antenna aperture resulting in lower efficiency and side lobe suppression, the effect of aperture blockage is negligible in presented concept. Moreover, owing to the subreflector, more suitable illumination distribution, i.e. higher gain and better side lobe suppression in H-plane can be achieved.

2 Concept

2.1 Radiating Elements

Radiating elements in the array are printed pentagonally shaped dipoles. One half of dipoles is printed on one side of the dielectric substrate and their other half on the opposite substrate side, Fig.1, [5]. These dipoles operate on the second resonance (antiresonance) enabling much slower impedance variation with frequency than in case of operation on the first resonance. The dipole impedance can range from about 70 Ω to a few hundred ohms. Variations of real and imaginary parts of the pentagonal dipole impedance with frequency are shown in Fig. 2. The dipole is optimized to impedance around (100 + j0) Ω at the central frequency of 26 GHz. Relative dielectric constant (ε_r) and thickness (h) of the substrate the dipole is printed on are 2.1 and 0.254 mm (CuFlon), respectively. Impedance variation

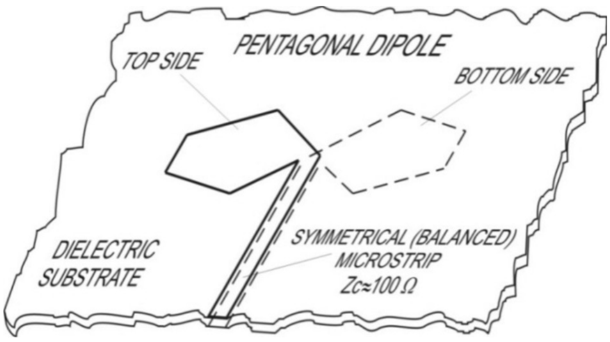

Figure 1: Printed pentagonal dipole as a basic element of the antenna array.

with frequency in such dipoles is a few dozen times smaller than in patches which are the most common conventional printed radiating elements. Bandwidth of the single dipole (VSWR < 2) is around 30 %.

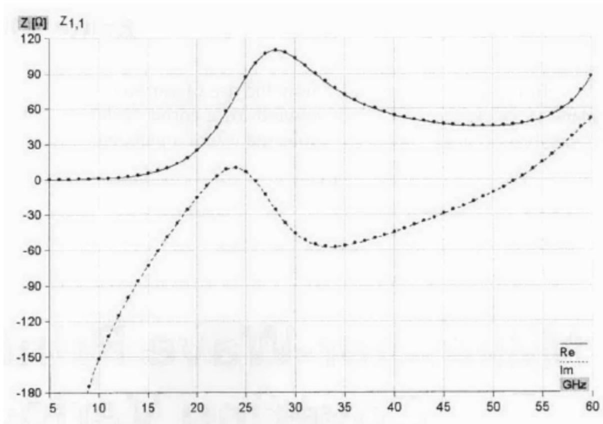

Figure 2: Real and imaginary parts of the pentagonal dipole impedance* as a function of frequency (ε_r=2.1, h =0.254 mm, S**= λ/4).

*The dipole impedance is optimized to obtain (100+j0) Ω at 26 GHz.
**S – distance between dipole axis and the flat reflector.

2.2 Axial Array of Dipoles

An axial array of dipoles has been formed, Fig. 3. Mutual impedances of these dipoles are relatively small which makes the design of the array significantly simpler which is especially important in cases of beam scanning. Certainly, the number of radiating elements in the array depends on the required E-field beamwidth. Distance between adjacent dipoles is practically a compromise between the gain and the sufficient suppression of grating lobes.

The distance between dipoles in axial antenna arrays with tapered feed distribution is chosen to be around 0.85 λ in order to obtain relatively high array gain and grating lobe level that is lower than the highest (usually the first) side lobe level, [6] (which is 13 dB suppressed with regard to the main lobe in case of uniform distribution).

2.3 Printed Subreflector

In front of the array of dipoles positioned on the focal axis of the cylindrical-parabolic reflector, there are strips printed on both sides of the substrate playing the role of a subreflector, Fig. 3, Fig. 5. Subreflector's axis and longitudinal axis of the dipoles' array are spaced λ/4 apart at the central frequency. Use of the subreflector offers the possibility of decreasing the depth of the cylindrical-parabolic reflector, i.e. of lowering the ratio L_f/D, where L_f is the focal length of the reflector and D is its width. Aperture blockage of the antenna structure by this subreflector is almost negligible due to extremely small thickness of the dielectric substrate (around λ/100). By varying width of the subreflector strip one can optimize illumination distribution of the cylindrical-parabolic reflector and obtain higher gain.

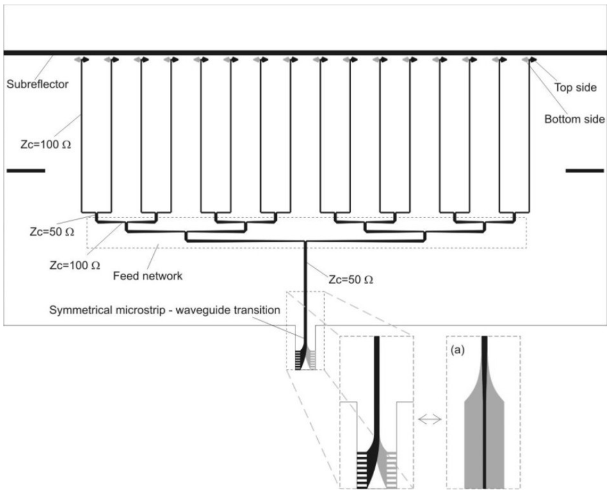

Figure 3: Printed antenna array with the subreflector and the feed network integrated on the same dielectric substrate.

2.4 Transition to Coaxial Connector or to Rectangular Waveguide

Complete feed network is realized in symmetrical (balanced) microstrip lines. In order to link a symmetrical to an asymmetrical (conventional) structure, a tapered symmetrical to asymmetrical microstrip transition (BAL-UN) is used in ranges below 40 GHz, Fig. 3(a). Its asymmetrical end is terminated with a coaxial SMA connector. However, in frequency ranges above 40 GHz there is a need for symmetrical microstrip-to-rectangular waveguide transition, [7]. Design of this transition is based on gradually tapering lines of a symmetrical microstrip that enters into waveguide and forming ridges at opposite sides of a dielectric substrate, Fig. 3. Through these ridges the E-field vector is being concentrated and rotated by 90° becoming parallel to shorter sides of a rectangular waveguide.

2.5 Cylindrical-Parabolic Reflektor

Cylindrical-parabolic reflector is made of a relatively thin aluminum (2 mm). It consists of two halves that are attached to each other along their apexes and fastened by screws or clasps. Holes through which symmetrical microstrip lines of the feed network pass are drilled through the junction of the two reflector's halves. Diameter (d) of these holes is chosen to be d>3W, where W is width of the symmetrical microstrip feed line, Fig 4. In this way the influence of the holes' rims on the feed line is being eliminated.

Ratio L_f/D (L_f – focal length of the reflector, D – width of the reflector) equals 0.2 in realized antennas while the length of the reflector (L) depends on the length of the axial array.

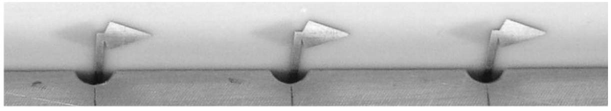

Figure 4: Holes in the cylindrical-parabolic reflector through which microstrip lines of the feed network pass.

2.6 Feed Network

Feed network is realized in symmetrical microstrip mainly for these reasons:

- Radiating elements are dipoles whose halves are printed on the opposite sides of the dielectric substrate thus representing a typical symmetrical structure.
- Feed networks in printed antenna structures are the main source of losses due to loss in feed lines. Symmetrical microstrip structure by its nature has lower losses than a conventional asymmetrical microstrip.

In realized antenna models with uniform feed distribution tapered impedance transformers are used in branching lines of the feed network, as shown in Fig 3. In case of antennas with high side lobe suppression we applied quarter-wave impedance transformers with suitable transformation ratio enabling desired tapered distribution, Fig 5.

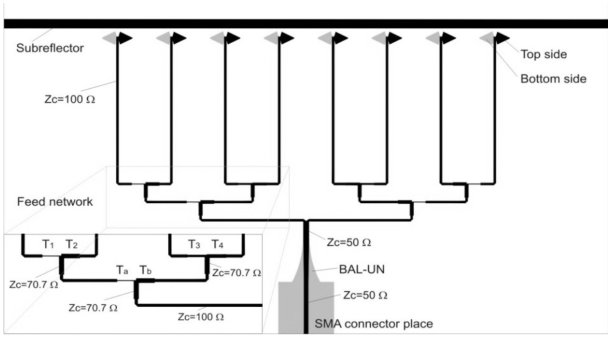

Figure 5: Example of feed network with impedance transformers (T_{1-4}, T_{a-b}) for tapered distribution (detail in the left lower corner).

Symmetrical microstrip feed networks are terminated either with symmetrical-to-asymmetrical microstrip transition or with symmetrical microstrip-to-wave-guide transition, both described in the subchapter 2.4.

3 Realizations

On the basis of new design concept and by use of WIPL-D software package [8] for simulations four models of printed antenna arrays in the cylindrical-parabolic reflector have been developed:

(A) Array with 8 radiating elements operating at 26 GHz range with uniform feed distribution,
(B) Array with 8 radiating elements operating at 26 GHz range with tapered feed distribution,
(C) Array with 16 radiating elements operating at 23 GHz range with uniform feed distribution, and
(D) Array with 16 radiating elements operating at 60 GHz range with uniform feed distribution.

Their main technical and measured electrical characteristics are given in Table 1 while the photographs of the realized models are shown in Figures 6 - 9.

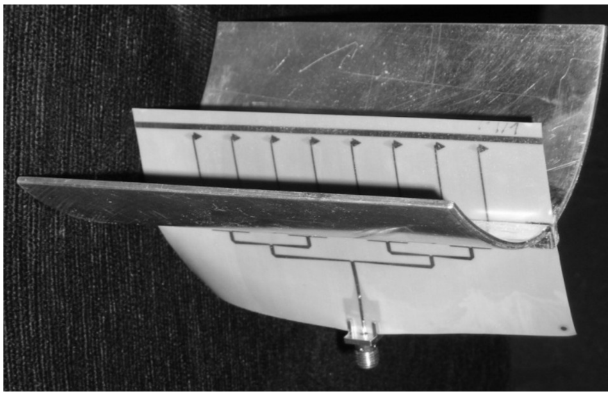

Figure 6: Photograph of the realized 26 GHz antenna array (A) in the cylindrical-parabolic reflector with uniform feed distribution.

From the obtained results we can come to a conclusion that practically all relevant parameters of this class of antenna arrays (bandwidth, gain, aperture efficiency) are significantly better than those of conventional printed antenna arrays.

Table 1

<table>
<tr><th colspan="2"></th><th colspan="2">Array (A)</th><th colspan="2">Array (B)</th><th colspan="2">Array (C)</th><th colspan="2">Array (D)</th></tr>
<tr><td colspan="2">Number of radiating elements</td><td colspan="2">8</td><td colspan="2">8</td><td colspan="2">16</td><td colspan="2">16</td></tr>
<tr><td colspan="2">Feed distribution</td><td colspan="2">Uniform</td><td colspan="2">Tapered</td><td colspan="2">Uniform</td><td colspan="2">Uniform</td></tr>
<tr><td colspan="2">Dielectric substrate</td><td colspan="2">CuFlon (εr=2.1, h=0.254 mm, tanδ=4x10-4)</td><td colspan="2">CuFlon (εr=2.1, h=0.254 mm, tanδ=4x10-4)</td><td colspan="2">CuFlon (εr=2.1, h=0.254 mm, tanδ=4x10-4)</td><td colspan="2">CuFlon (εr=2.1, h=0.127 mm, tanδ=4x10-4)</td></tr>
<tr><td colspan="2">Dipoles' impedances</td><td colspan="2">~(100+j0) Ω</td><td colspan="2">~(100+j0) Ω</td><td colspan="2">~(100+j0) Ω</td><td colspan="2">~(100+j0) Ω</td></tr>
<tr><td colspan="2">Distance between dipoles</td><td colspan="2">11 mm (0.95 λ, 26 GHz)</td><td colspan="2">10 mm (0.85 λ, 26 GHz)</td><td colspan="2">14 mm (1.07 λ, 23 GHz)</td><td colspan="2">5.5 mm (1.1 λ, 60 GHz)</td></tr>
<tr><td colspan="2">Width of the subreflector</td><td colspan="2">1.7 mm</td><td colspan="2">1.7 mm</td><td colspan="2">3.1 mm</td><td colspan="2">0.866 mm</td></tr>
<tr><td rowspan="2">Dimensions of the cylindrical-parabolic reflector</td><td>L (Length)</td><td colspan="2">110 mm</td><td colspan="2">110 mm</td><td colspan="2">250 mm</td><td colspan="2">100 mm</td></tr>
<tr><td>D (Width)</td><td colspan="2">100 mm</td><td colspan="2">100 mm</td><td colspan="2">200 mm</td><td colspan="2">100 mm</td></tr>
<tr><td colspan="2">Length of the BAL-UN/sym. mstrip to waveguide transition (case D)</td><td colspan="2">8 mm</td><td colspan="2">8 mm</td><td colspan="2">8 mm</td><td colspan="2">5.09 mm</td></tr>
<tr><td colspan="2">Type of connector</td><td colspan="2">SMA</td><td colspan="2">SMA</td><td colspan="2">SMA</td><td colspan="2">waveguide WR-15</td></tr>
<tr><td colspan="2">Measured gain at the central frequency</td><td colspan="2">~27.5 dBi (@26 GHz)</td><td colspan="2">~25.7 dBi (@26 GHz)</td><td colspan="2">~33 dBi (@23 GHz)</td><td colspan="2">~34 dBi (@60 GHz)</td></tr>
<tr><td>FSLSE* (measured)</td><td>FSLSH* (measured)</td><td>~13 dB</td><td>~20 dB</td><td>~28 dB</td><td>~22 dB</td><td>~13 dB</td><td>~14 dB</td><td>~13 dB</td><td>~17 dB</td></tr>
<tr><td colspan="2">Bandwidth (VSWR<2)</td><td colspan="2">(24.5-28.0) GHz</td><td colspan="2">(24.2-29.2) GHz</td><td colspan="2">(18-28) GHz</td><td colspan="2">(57.5-75.0) GHz</td></tr>
<tr><td colspan="2">Aperture efficiency</td><td colspan="2">54.1%</td><td colspan="2">35.8%</td><td colspan="2">54.2%</td><td colspan="2">54.2%</td></tr>
<tr><td colspan="2">Losses in metallization and dielectric</td><td colspan="2">~1.1 dB</td><td colspan="2">~1.1 dB</td><td colspan="2">~2.2 dB</td><td colspan="2">near 3 dB</td></tr>
<tr><td colspan="2">maximum handling power, theory/real</td><td colspan="2">~67 W / 33 W</td><td colspan="2">~67 W / 33 W</td><td colspan="2">~67 W / 33 W</td><td colspan="2">~20 W / 10 W</td></tr>
</table>

$FSLS_E^*$, $FSLS_H^*$ - First Side Lobe Suppression in E- and H-plane

Maximum working temperature for CuFlon is 175^{0}C, 150^{0}C above normal temperature of 25^{0}C. Substrate CuFlon is a soft substrate with low thermal conductivity, 0.25 W/m/^{0}C, comparing to high thermal conductivity silicon [11].

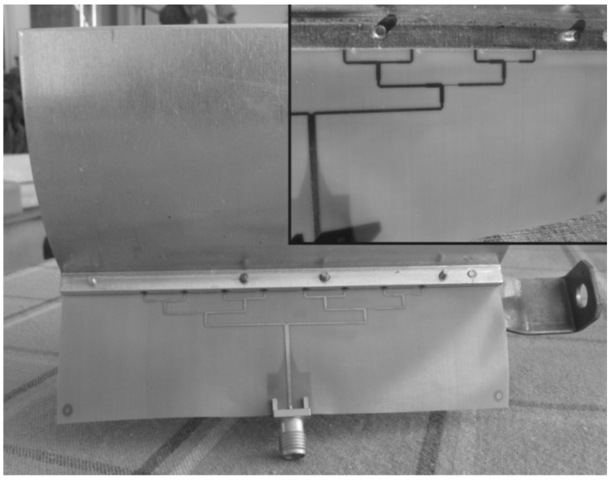

Figure 7: Photograph of the realized 26 GHz antenna array (B) in the cylindrical-parabolic reflector with tapered feed distribution with the detail of the tapered feed network.

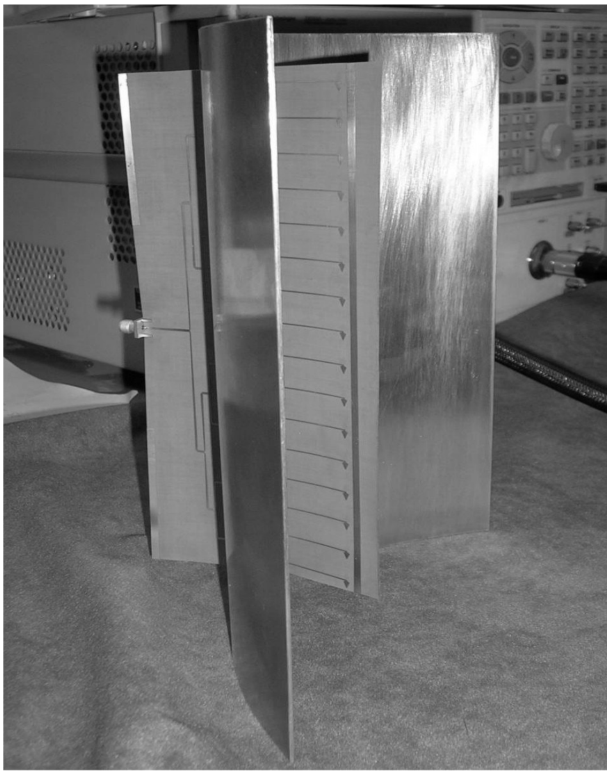

Figure 8: Photograph of the realized 23 GHz antenna array (C) in the cylindrical-parabolic reflector with uniform feed distribution.

Figure 9: Photograph of the realized 60 GHz antenna array (D) in the cylindrical-parabolic reflector with uniform feed distribution.

4 Conclusion

The paper proposes a new class of printed antenna structures that have most of advantages of printed antennas: high reproducibility, low weight, compactness, possibility of simple integration with other passive and active microwave circuits as well as low manufacturing cost. At the same time they feature high gain and relatively low losses which is not common for planar printed antenna arrays. The only disadvantage comparing to standard planar (2D) antenna structures is the third dimension, i.e. thickness, due to presence of the cylindrical-parabolic reflector. Four realizations of printed antenna arrays in cylindrical-parabolic reflector intended for various frequency ranges are presented, including antenna with high side lobe suppression for higher microwave ranges and antenna operating in millimeter range (57.5–75.0) GHz. Besides, proposed antenna structures are suitable for applications in beam scanning antennas as well as for forming the desired radiation pattern (for example, cosec^2). Experimentally obtained results are in good agreement with those obtained by simulation.

Acknowledgment

The authors would like to thank colleagues Ms. M. Marjanović, Ms. M. Pesić, Mr. N. Tasić, Mr. M. Tasić and Mr. Lj. Radović for their help in realization of the antenna models. This work has been supported by the Serbian Ministry of Education and Science within the Technological Development Project TR 32024.

References

1. A. Nesic, I. Radnovic, "High Gain Millimeter Wave Antenna with Cylindrical-Parabolic Reflector", TELSIKS 2009, Nis, Conference Proc. pp. 376-379
2. A. Nesic, I. Radnovic, "New Type of Millimeter Wave Antenna with High Gain and High Side Lobe Suppression", Optoelectronics and Advanced Materials – Rapid Communications Vol. 3, No.10, October 2009, pp. 1060-1064.
3. A. Nesic, I. Radnovic, "60 GHz Range High Gain Printed Antenna Array with a Cylindrical-Parabolic Reflector", Frequenz, 3-4/2010, Vol. 64 March/April 2010, 48-51.
4. A. Nesic and D. Nesic, "Cylindrical-Parabolic Antenna Fed by Printed Axial Array Like Primary Radiator", Patent Pending no. P-207/0738, 24. Sep. 2007
5. A. Nesic, Z. Micic, S. Jovanovic, I. Radnovic , D. Nesic, "Millimeter Wave Printed Antenna Arrays for Covering Various Sector Width", IEEE Antennas and Propagation Magazine, Vol.49, No.1, Feb. 2007, pp. 113-118
6. M. Mikavica, A. Nesic, CAD for Linear and Planar Antenna Array of Various Radiating Elements, ARTECH House, Norwood, MA, 1992
7. J. H. C. van Heuven, "A New Integrated Waveguide-Microstrip Transition", IEEE Transactions on MTT, vol. 24, 1976, pp. 144-147
8. *WIPL-D software package*, http://www.wipl-d.com/, WIPL-D d.o.o.: Belgrade, Serbia, 2012
9. M. Petersson, *Microstrip Solution for Innovative Microwave Feed Systems,* Department of Science and Technology, Linkoping University, Sweden, 2001
10. Rogers Corporation, MWI-2010, Calculator
11. D. Nesic, I. Jokic, M. Frantlovic and M. Sarajlic, "Wide Band-stop Microwave Microstrip Filter on High-resistivity Silicon", MIDEM - Journal of Microelectronics, Electronic Components and Materials, vol. 42, no. 4, 2012, pp. 282-286

Arrived: 26. 02. 2013
Accepted: 08. 04. 2013